Spatial changes in soil stable isotopic composition in response to carrion decomposition

Sarah W. Keenan[1,2], Sean M. Schaeffer[1], and Jennifer M. DeBruyn[1]

[1] University of Tennessee, Department of Biosystems Engineering and Soil Science, 2506 E.J. Chapman Drive, Knoxville, TN 37996

[2] Current address: South Dakota School of Mines and Technology, Department of Geology and Geological Engineering, 501 E. St. Joseph Street, Rapid City, SD 57701

Corresponding authors: sarah.keenan@sdsmt.edu, jdebruyn@utk.edu

Abstract

Decomposition provides a critical mechanism for returning nutrients to the surrounding environment. In terrestrial systems, animal carcass, or carrion, decomposition results in a cascade of biogeochemical changes. Soil microbial communities are stimulated, resulting in transformations of carbon (C) and nitrogen (N) sourced from the decaying carrion soft tissues, changes to soil pH, electrical conductivity, and oxygen availability as microbial communities release CO_2 and mineralize organic N. While many of the rapid changes to soil biogeochemistry observed during carrion decomposition return to background or starting conditions shortly after soft tissues are degraded, some biogeochemical parameters, particularly bulk soil stable $\delta^{15}N$ isotopic composition, have the potential to exhibit prolonged perturbations, extending for several years. The goal of this study was to evaluate the lateral and vertical changes to soil stable isotopic composition one year after carrion decomposition in a forest ecosystem. Lateral transects extending 140 cm from three decomposition "hotspots" were sampled at 20 cm intervals, and subsurface cores were collected beneath each hotspot to a depth of 50 cm. Bulk soil stable isotopic composition ($\delta^{15}N$ and $\delta^{13}C$) indicated that one year after complete soft tissue removal and decay, soils were significantly ^{15}N-enriched by 7.5 ± 1.0 ‰ compared to control soils up to 60 cm from the hotspot center, and enrichment extended to a depth of 10 cm. Hotspot soils also contained 10 % more N compared to control soils, indicating that decomposition perturbs N pools. Our results demonstrate that carrion decomposition has the potential to result in long-term changes to soil biogeochemistry, up to at least one year after soft tissue degradation, and to contribute to bulk soil stable isotopic composition.

1 Introduction

Nutrient hotspots form from the introduction of carbon (C) and nitrogen (N)-rich compounds into an ecosystem, resulting in elevated reaction rates compared to surrounding regions (McClain et al., 2003). For terrestrial and aquatic systems, hotspots may be sourced from fallen trees (Lodge et al., 2016), annual deposition of deciduous leaves (Vidon et al., 2010), animal scat (Erskine et al., 1998; van der Waal et al., 2011), or animal carcasses (Parmenter and Lamarra, 1991; Carter et al., 2007; Wheeler et al., 2014; Wheeler and Kavanagh, 2017). Hotspots sourced from animal carcasses, also referred to as carrion hotspots, significantly alter surface and belowground soil physiochemistry and plant communities in terrestrial ecosystems (Carter et al., 2007; Keenan et al., 2018a). These alterations can have significant long-term impacts; for example, large animal carcasses had measurable effects on a prairie ecosystem for at least 5 years (Towne, 2000), and a decade or more in the Arctic (Danell et al., 2002). In addition to providing a critical source of C and N, carrion hotspots are important sources of ecosystem heterogeneity (Towne, 2000; Bump et al., 2009b) and promote biodiversity (Barton et al., 2013).

Carrion decomposition occurs in a series of physical (Payne, 1965) and biogeochemical (Keenan et al., 2018a) stages. The breakdown and release of animal tissues provides a labile source of nutrients for insect and vertebrate scavengers as well as soil microfauna and microbiota (i.e., nematodes, bacteria, fungi). Studies evaluating the consequences of carrion decay on soil biogeochemistry have monitored decomposition on a range of timescales, from days (Metcalf et al., 2013; Macdonald et al., 2014; Keenan et al., 2018a; Szelecz et al., 2018) to years (Towne, 2000; Bump et al., 2009a; Keenan et al., 2018b), and in different climatic and geographic settings, including temperate forests (Melis et al., 2007; Cobaugh et al., 2015; Keenan et al., 2018a) and Australian rangeland (Macdonald et al., 2014), as well as under controlled laboratory

settings (Carter et al., 2008, 2010). Some of the key changes that occur in soils following the deposition and decomposition of carrion include: changes to pH (both increases and decreases), increased electrical conductivity, decreased oxygen availability, increased gas fluxes (CO_2, CH_4, N_2O, H_2S), elevated rates of microbially-driven C and N cycling, and increased dissolved compounds available to microbes (NH_4^+, NO_3^-, Ca^{2+}, SO_4^{2-}) (Melis et al., 2007; Aitkenhead-Peterson et al., 2012; Keenan et al., 2018a).

Many of the rapid, pulsed perturbations to soil C and N pools observed at carrion hotspots, such as elevated microbial respiration rates (measured as CO_2 release) and changes to soil pH, return to background biogeochemical conditions during the skeletal stage of decomposition, when soft tissues have been largely or completely degraded by insect and vertebrate scavengers (Cobaugh et al., 2015; Keenan et al., 2018a). However, certain biogeochemical measures, including soil stable $\delta^{15}N$ composition, have been observed to remain enriched in soils collected at carrion hotspots compared to background soils for a protracted period of time, up to several years (Bump et al., 2009a ; Wheeler and Kavanagh, 2017). Soil stable isotopic composition integrates all biogeochemical activity within the soil as well as inputs from plant or animal matter. In contrast with $\delta^{15}N$ enrichment, no changes in soil $\delta^{13}C$ composition have been observed in surface soils of decomposition hotspots (Wheeler and Kavanagh, 2017; Keenan et al., 2018a). A variety of studies have demonstrated the potential for natural abundances of ^{15}N to be used as a tracer of ecological processes, including N input from animals (urea and feces) in N-limited and isolated ecosystems (Erskine et al., 1998) and input of marine taxa (salmon carcasses) to terrestrial and riparian areas (Kline et al., 1990; Koyama et al., 2005).

While ^{15}N enrichment due to carrion decomposition has been demonstrated in previous work, these studies were limited to surface soils (maximum sampling depth of 10 cm) from the center of the hotspots (Bump et al., 2009a; Wheeler and Kavanagh, 2017). This has left a gap in our understanding of the spatial extent of carcass enrichment, which is ultimately necessary for quantifying ecosystem impacts of these decomposition inputs. Given the potential for natural abundance ^{15}N to serve as a long-term tracer of decomposition processes, the goal of this study was to evaluate spatial changes in stable ^{15}N-enrichment at a carrion hotspot one year post-decay. In particular, the lateral and vertical extent of stable isotope changes as a result of enhanced biogeochemical reactions in a hotspot is largely unknown. Soils beneath and adjacent to former carrion hotspots (up to ~40 cm, the extent of visible fluid migration) were expected to remain ^{15}N-enriched one year after decay. Additionally, isotopic enrichment was expected to persist to at least 10 cm depth, the maximum depth examined in previous studies.

2 Materials and Methods

2.1 Study area and sample collection

The study site was a mixed deciduous forest in East Tennessee (36°0'1.0" N, 84°13'1.6" W, ~330 m elevation). Soils were part of the Fullerton-Pailo complex and characterized as Typic Paleudults (Soil Survey Staff, 2018). The A horizon extended to approximately 20 cm depth. Five ~23 kg nuisance North American beaver (*Castor canadensis*) carcasses were placed frozen within scavenger prevention enclosures (1.19 x 0.74 x 0.81 m) and allowed to decay naturally, starting 31 July 2016. As part of a separate study, approximately 75 g of surface soil (0-5 cm depth) was collected a total of five times during decay beneath each animal (Keenan et al., 2018a). For this study, soils were collected on 8 August 2017, one year after decomposition, and

after bones had been removed from the site. Soils were taken from surface transects as well as from cores obtained at depth below three carrion hotspots. Approximately 30 g of soil from the top 0-5 cm were collected using a 3 cm diameter auger within the hotspot—an elliptical area 40 to 80 cm in diameter of visibly discolored soil (Figs. 1, 2). Surface samples were additionally collected along a linear transect radiating perpendicular from the longest axis of the elliptical hotspot at 20 cm intervals up to 140 cm (Fig. 1). Within the hotspots, soils were cored to a depth of 50 cm using a 10 cm diameter auger; cores were partitioned into depth intervals of 0-5, 5-10, 10-15, 15-20, 20-30, 30-40, and 40-50 cm depth (Fig. 1).

All soil samples were homogenized to a uniform consistency in the field by hand (changing nitrile gloves between samples), removing any rocks, roots, leaves, or vegetation larger than 2 mm. Samples were transported to the lab and processed immediately. Aliquots were oven-dried in triplicate at 105°C for 48 h to determine gravimetric moisture (Table 1, Table S1). Once dried, subsamples were powdered in an agate mortar and pestle and stored in 1.5 mL tubes until subsequent isotopic analyses. Samples (~25 mg for surface soils; ~50 mg for soils below 20 cm depth) were transferred into 5 × 9 mm tin capsules (Costech). Isotopic analyses were conducted at Washington University in St. Louis. Samples, standards, and blanks were loaded into a Costech Zero Blank autosampler and combusted in a Flash 2000 elemental analyzer. Soil $\delta^{13}C$ and $\delta^{15}N$ values were measured on a Delta V Plus continuous-flow (Conflo IV, Thermo Fisher Scientific), isotope-ratio-mass spectrometer. Standards included millet and acetanilide. Millet was used to evaluate linearity. Sample carbon isotopic values were corrected for sample size and instrument drift using millet and acetanilide, and nitrogen values were corrected using millet, acetanilide, and urea. Analytic precision was <0.2 ‰ for both carbon and nitrogen. Results are presented in δ notation as parts per mil (‰) where $\delta^{13}C = [(({}^{13}C/{}^{12}C_{sample} \div$

$^{13}C/^{12}C_{standard}) - 1) \times 1{,}000]$ and $\delta^{15}N = [((^{15}N/^{14}N_{sample} \div {}^{15}N/^{14}N_{standard}) - 1) \times 1{,}000]$. Vienna Pee Dee Belemnite was used as the carbon standard and air was used for nitrogen.

Soils collected from the center (0-5 cm depth) of all five hotspots and a composite control sample (pooled soil collected from five locations ~3 m from each hotspot) were also analyzed for microbial respiration rates (as evolved CO_2), ammonium, nitrate, nitrification potential, pH, electrical conductivity, dissolved organic C and N, and protein content, building from a previous study at the site and following the methods described by Keenan et al. (2018a). In brief, headspace CO_2 was measured immediately after placing and sealing soil into 60 mL serum vials, as well as after 24 h (LI-820, Licor Inc.). Vacuum-filtered (1 μm; Ahlstrom, glass microfiber) soil extracts (10 g soil: 40 mL 0.5 M K_2SO_4) were collected after shaking for 4 hours at 150 rpm at room temperature, and were frozen at -20°C until subsequent colorimetric analysis of ammonium and nitrate (Rhine et al., 1998; Doane and Horwath, 2003). Aliquots were oxidized with a persulfate solution to measure dissolved organic carbon (DOC) as evolved CO_2 and dissolved organic nitrogen (DON) colorimetrically as nitrate (Doyle et al., 2004). Nitrification potential was determined colorimetrically using a modified chlorate block method optimized for microplates (Belser and Mays, 1980; Keeney and Nelson, 1982; Hart, 1994). Soil pH and electrical conductivity were measured from a soil slurry (3 g soil: 6 mL deionized water) using a handheld multi-parameter meter (Orion A329, Thermo Scientific). Protein content was determined using the Bradford Assay (Wright and Upadhyaya, 1996; Redmile-Gordon et al., 2013). Because the goal of this study was to focus specifically on stable isotopes as long-term tracers in carrion hotspots, only surface soils from the five remnant hotspot centers were processed for full physiochemistry.

2.2 Stable isotope analyses

The contribution of carcass-derived nitrogen to bulk soil stable isotopic composition in surface transects was determined using a linear two-member isotope mixing model (Wheeler and Kavanagh, 2017; Keenan et al., 2018a), using bulk control soil $\delta^{15}N$ composition (0.1 ‰) as one end-member and beaver decomposition fluid (10.2 ‰) as the other. Decomposition fluid is the by-product of microbial and autolytic processes acting on a carcass after animal death. Fluids consist of amino acids, dead and live microbial cells, urea, water, and lipids, and represent one of the primary mechanisms for return of host's tissues to the surrounding environment. Decomposition fluid isotopic composition was previously determined, using fluids collected from three decomposing beavers left on a shallow plastic tray to intercept fluids (Keenan et al., 2018a). The linear equation for the isotope mixing model (Wheeler and Kavanagh, 2017) was defined as:

$$CDN = [(TEM - SEM)/(FEM - SEM)] \times 100$$

Where CDN is the carcass-derived N (%), TEM is the average $\delta^{15}N$ of soil from the treatment condition (sampling interval along the surface transects), SEM is the end-member control soil stable isotopic composition (0.1 ‰), and FEM is the end-member isotopic composition of decomposition fluids (10.2 ‰). The contribution of control soil-derived $\delta^{15}N$ to measured treatment conditions was calculated by subtracting CDN (%) from 100 %.

To track changes in $\delta^{15}N$ between surface soil and soil collected at depth, $\Delta^{15}N$ values were calculated by subtracting the $\delta^{15}N$ value of soil at each depth from values obtained at the surface of the hotspot and control sampling locations. Negative $\Delta^{15}N$ values indicate that surface soils are ^{15}N-enriched compared to soils at depth (Martinelli et al., 1999).

2.3 Statistical analyses

Data were analyzed using SigmaPlot to test for significant differences between treatments and controls. For both surface and depth transects, data from the three transects were treated as replicates for subsequent statistical analyses. Significance ($p < 0.05$) was determined based on one-way ANOVA analyses with Holm-Sidak post-hoc testing. Significant differences between control and hotspot soils were determined using paired t-tests at each sampling depth or transect interval using R (R Core Team, version 3.5.0).

3 Results

3.1 Surface soil biogeochemical changes during decomposition

During carrion decomposition, fluids sourced from the carcass were released into the surrounding environment (Fig. 2). The pulse of nutrient-rich fluids resulted in significant long-term changes to surrounding soil physiochemistry following fluid degradation by soil microbial communities (Table 1, Table S1). In particular, after one year of decay, soil pH was significantly lower than control, initial, and pre-decay soils ($p < 0.001$; $F = 59.317$). In addition, bulk soil $\delta^{15}N$ remained significantly enriched compared to control and starting soil isotopic composition ($p < 0.001$; $F = 27.948$). Other physicochemical parameters, including conductivity, microbial respiration, DOC, DON, ammonium, nitrate, and nitrification potential all returned to background conditions after one year. With the exception of the one year samples, data were previously published in Keenan et al. (2018a) and are included here for comparison.

3.2 Lateral changes in stable isotopic composition

Soils were significantly ^{15}N-enriched within the visible carrion hotspot (mean soil composition 7.5 ± 1.0 ‰) and up to 60 cm from the hotspot center (2.2 ± 0.5 ‰) compared to composite control soils (0.1 ‰) (Fig. 3, Table S2) (paired t-test, $p = 0.016$). Soil $\delta^{15}N$ values gradually declined, reaching background abundance values around 80 cm from the hotspot center. In contrast, there were no significant differences between control and hotspot soil $\delta^{13}C$, and no differences as a function of distance from the hotspot center (one-way ANOVA, $p = 0.464$; $F = 1.004$). C/N ratios were lower within the hotspot and exhibited a gradual and significant increase with increasing distance from the hotspot center (Fig. 3). However, there were no significant differences between hotspot and control soil C/N.

The influence of carrion decomposition on soil stable $\delta^{15}N$ isotopic composition decreases with increasing distance from the hotspot (Figs. 3a, S1). Soil C/N composition follows a linear trend, increasing by 0.07 per cm from the hotspot center (Fig. S1). Based on linear two-member isotope mixing models, carcass-derived fluids exhibit a linear decrease in contribution to soil isotopic composition with increasing distance from the hotspot. Carcasses contribute to soil stable $\delta^{15}N$ isotopic composition up to 60 cm from the hotspot center (Fig. 4), an area that was beyond the decomposition island and was not visibly discolored (Fig. 2).

3.3 Vertical changes in stable isotopic composition

Soil collected at depth beneath the three mortality hotspots was significantly ^{15}N-enriched compared to control soils up to 10 cm depth (Fig. 5). Surface hotspot soils were also enriched at 30 cm depth compared to the control. Control soils became more ^{15}N-enriched with increasing depth. There was no significant difference between control and hotspot soil $\delta^{13}C$ and C/N values,

and both exhibited the same trends with depth. Soils exhibited ^{13}C-enrichment with increasing depth and a decline in C/N ratios.

Control soils exhibited a strong positive linear relationship between the negative of the natural log of bulk soil %N and stable isotopic composition, reflecting decreasing N and C availability with increasing depth. Decomposition results in a shift in the observed hotspot soil N isotopic discrimination (*D*, or the slope of the linear regressions) (Natelhoffer and Fry, 1988), leading to a breakdown of a strong linear relationship compared to control soils (Fig. 6). *D* does not change for C isotopes in control or hotspot soils.

In general, soils exhibit a trend of increasing $\Delta^{15}N$ (the difference between soil $\delta^{15}N$ value at a specific depth and $\delta^{15}N$ at the surface) with depth, reflecting ^{15}N-enrichment in deep forest soils (Martinelli et al., 1999). Hotspot soils exhibited lower $\Delta^{15}N$ values compared to control soils, indicating little change in ^{15}N-enrichment with depth (Table 2). Control soils displayed increasing $\Delta^{15}N$ with depth, a pattern globally observed in forest soils (Martinelli et al., 1999) (Table 2). Combined with *D* (Fig. 6), hotspot and control vertical profiles have distinct N sources and exhibit distinct N pools with depth.

Soils collected from 0-5 cm exhibited a significant contribution from decomposition fluids (Fig. 5). As depth increases beyond 10 cm, there is no change to the proportional contribution of decomposition fluid to bulk stable isotopic composition. By 30-40 and 40-50 cm depth, hotspot soil $\delta^{15}N$ and $\delta^{13}C$ compositions are similar to control soils (Fig. 5), indicating limited, if any, input from decomposition fluids.

4 Discussion

Soils associated with carrion decomposition hotspots retained biogeochemical markers of vertebrate decay at least one year after soft tissue degradation. Within the hotspots, soils remained ^{15}N-enriched compared to control locations. At this specific location and soil type, decomposing animals have the potential to exert long-term changes, here at least one year, on surface and subsurface soil stable isotopic composition. The beaver carcasses used in this study, which were between 20 kg and 25 kg in mass, resulted in measurable changes to soil biogeochemistry down to 10 cm depth and up to 60 cm away from the hotspot center, beyond the area that was visibly discolored from decomposition fluids. The total %N measured in soils can be used to approximate the contribution of beaver N to soil. During active decomposition, hotspot soils contained 36 % more N compared to control soils (0.362 % N vs. 0.267 %). After one year, hotspot soils still contained 10 % more N than control soils (0.285 % N vs. 0.260 %), reflecting a loss of ~28 % of the beaver-derived N in one year. Based on prior calculations, each beaver introduced approximately 0.47-0.79 kg N and 2.7-4.6 kg C to the soil (Keenan et al., 2018a). After one year, approximately 0.1-0.2 kg N derived from the carcass remains within the soil.

The linear two-member isotope mixing model indicates that the contribution of carcass-derived fluids to soil isotopic composition decreases with increasing distance from the hotspot (Fig. 4). However, the observed isotopic enrichment likely reflects a contribution of a ^{15}N-enriched input (carcass fluid) as well as subsequent diagenetic fractionation driven by soil microorganisms. It is likely that the elevated N availability provided by a decomposing carcass would result in additional nitrification and denitrification, which would increase the $\delta^{15}N$ independent of source mixing. Nitrification potential rates were elevated during earlier stages of decomposition, but were not different from control soils after 1 year (Table 1). The two-member

mixing model assumes a simple mixing of soil and carcass-derived N, but diagenetic fractionation is also likely involved in the observed $\delta^{15}N$ patterns along the surface transects.

The contribution of carcass-derived N to soils at depth as well as laterally is influenced by a variety of physical and climatic variables. Here, decay occurred during the summer in East Tennessee, with an average high of 32.2°C for the month of August. Carcasses were exposed to measurable precipitation six out of 10 days after placement, preventing soft tissues from significant desiccation and supporting abundant blowfly larvae and other insect activity. Blowfly larvae migrating away from the carcasses on the surface and within the soil to pupate likely provided an important physical mechanism to distribute beaver-enriched N to surrounding soils. Blowfly larvae can move up to 10 m away from the carcass, and typically extend down into the soil up to 10 cm depth, depending on the soil substrate properties (Gomes et al., 2006). As blowfly larvae disperse, they have the potential to physically transport decomposition fluids acquired internally or externally during feeding, release excrement during migration, or die, leaving their tissues to degrade. An estimated 66 % of pupae that disperse to pupate die en route (Putman, 1977). Rainfall may have also contributed to the downward movement of decomposition fluids.

The temporal persistence of isotopic enrichment hotspots is currently unknown, but is likely to be ecosystem, carrion type, and carrion mass-specific. A larger carcass would be expected to result in greater lateral and vertical dispersal of carrion-derived fluids, as well as greater changes to ecosystem processes, because of the greater volume of decomposing soft tissue (Baruzzi et al., 2018). In addition, larger carcasses may host a larger and longer-lived insect community (Parmenter and MacMahon, 2009), including blowfly larvae, which may further nutrient dispersal and may impact a larger area. Bump et al. (2009b) observed elevated

foliar $\delta^{15}N$ values in plants growing on sites impacted by deer carcass (~56 kg) decomposition at least 2.5 years after decay in a temperate hardwood forest, suggesting a long-lived hotspot signature. In some ecosystems, such as the Arctic tundra, isotopic enrichment is likely to persist for even longer based on perturbations to C and N surrounding muskox after 5 to 10 years of decay (Danell et al., 2002).

Increasing $\delta^{13}C$ and $\delta^{15}N$ values with depth in soils has previously been observed in a variety of soil types and climatic conditions (Natelhoffer and Fry, 1988; Martinelli et al., 1999; Billings and Richter, 2006). Changes to $\delta^{13}C$ with depth are due to progressive cycling of C through microbial biomass (Liang et al., 2017), where selective preservation and biochemical fractionation together lead to ^{13}C-enriched organic C in soil (Natelhoffer and Fry, 1988; Billings and Richter, 2006). While we observed a similar increase in $\delta^{13}C$ with depth, we did not see a significant change in ^{13}C as a result of carcass enrichment. Wheeler and Kavanagh (2017) similarly did not observe a change in soil $\delta^{13}C$ following carrion decomposition, which may be due to the degradation of carcass-derived C (and uptake by microbes and blowfly larvae) combined with elevated background C in soil compared to N.

Increasing $\delta^{15}N$ values with depth reflects two broad biochemical processes leading to fractionation, both likely driven by microbial activities. First, the preferential excretion of ^{15}N-depleted compounds during catabolism and anabolism leaves the residual microbial cells and soil ^{15}N-enriched. Second, kinetic fractionation associated with gaseous N loss is also known to result in enrichment, depending on the microbial communities present and N mineralization rates (Evans, 2001; Robinson, 2001; Liang et al., 2017). Over time, as soil profiles develop, accretion of ^{15}N-enriched microbial cells, particularly fungi, leads to isotopic enrichment at depth (Billings and Richter, 2006). In contrast, plant and leaf litter are the dominant contributors to N pools in

surface soils in most temperate forest ecosystems (Vidon et al., 2010), resulting in surface soils that are isotopically-depleted compared to the soils at depth. Decomposition hotspots, however, disrupt the expected pattern (Fig. 5), causing surface enrichment, and likely leave a lasting impact on soil stable isotopic composition.

For systems at or near steady state conditions, the difference in isotopic enrichment between soils at depth and the surface ($\Delta^{15}N$) provides a way to compare soils from different geographic and climatic locations (Martinelli et al., 1999), and was used here to compare hotspot soils and those collected at control locations. $\Delta^{15}N$ values observed in the control depth profile are within the expected range observed in temperate forests worldwide (2.7 to 9.1 ‰) (Table 2). However, as a consequence of carrion inputs and decay, $\Delta^{15}N$ values are more similar to those observed in tropical forest ecosystems (1.1 to 4.3 ‰). In tropical systems, lower $\Delta^{15}N$ values are thought to reflect more open N cycling with elevated N losses (nitrification, nitrate leaching, and ammonia volatilization) under conditions of elevated total N inputs (Martinelli et al., 1999). Whether our observed changes in $\Delta^{15}N$ are due to elevated N cycling rates, disequilibrium effects across the soil profile due to changing N inputs from a system dominated by atmospheric dry and wet deposition of nitrate and ammonium to one with carrion-sourced N, or both, is not known.

The observed stable isotopic discrimination (*D* or the slope of the linear regressions) did not differ for control and hotspot soil $\delta^{13}C$ (Fig. 6), suggesting that C cycling and pools in soils one year after carrion decay are not altered. In contrast, *D* values for $\delta^{15}N$ were different between control and hotspot soils, which reflects a loss of the linear relationship and indicates distinct N sources for the two soil profiles. This also emphasizes that decaying carrion provide an important and potentially distinct N pool for soil ecosystems that have the potential to mask natural (background) processes that control soil profile ^{15}N gradients with depth. In addition, differences

in *D* values between the two soils suggest that there may be less discrimination occurring within hotspot soils compared to control soils, likely due to the rapid input of an isotopically-enriched N pool (Evans, 2001).

Hotspot soils received the input of beaver-derived fluids (10.2 ± 0.4 ‰) (Keenan et al., 2018a) as well as soft and hard tissues (1.0 to 4.0 ‰ for beaver bone collagen from Minnesota; Fox-Dobbs et al., 2007). Stable isotopic composition of surface soils strongly suggests that decomposition fluids are a significant contributing source to bulk soil stable isotopic composition up to 60 cm from the hotspot center (Fig. 4), and $\delta^{15}N$ enriched values in the soil profile at depth also suggest some contributions up to 10 cm depth (Fig. 5). Beyond 10 cm depth, control soils and hotspot soils are indistinguishable, suggesting that decomposition fluids do not significantly influence soil stable isotopic composition. Rather, natural $\delta^{15}N$ enrichment due to soil accretion processes can explain the observed soil stable isotopic composition.

5 Conclusions

The decay of ~23 kg North American beavers resulted in rapid (within days) and long-lived (up to one year) ^{15}N-enrichment in forest soils up to 10 cm depth and ~60 cm distal. Observed ^{15}N-enrichment at depth and laterally is likely due to a combination of physical movement of fluids during decomposition and the transport of fluids by insects, particularly blowfly larvae. In this system, rainfall during decomposition may have also acted as a physical transport mechanism. While likely to be significantly influenced by carcass size, climate, and soil type, decomposition has the potential to exert long-lived influences on soil stable isotopic composition.

Data availability

All data generated in this study are available in the Supplement.

Author contributions. SWK and JMD designed the experiments. All authors assisted with data interpretation. JMD and SMS provided financial, lab, and analytical resources. SWK and JMD prepared the manuscript with contributions from SMS.

Competing interests. The authors declare that they have no conflict of interest.

Acknowledgements. Salvaged nuisance beavers were provided by the USDA, APHIS, Wildlife Services of East Tennessee. Lois S. Taylor, Jose Liquet, Fei Yao, and Jialin Hu assisted with soil collection. Alex Bradley provided lab and instrument access, and Melanie Suess assisted with stable isotopic analyses. Three reviewers are thanked for their constructive feedback that greatly improved this manuscript. This research was funded by a National Science Foundation Award (1549726) to JMD and SMS.

Figure and table legends

Figure. 1: Schematic cross-section view of the locations of soil samples (stars) collected from each of three carrion decomposition sites. Dashed line represents the hotspot—the area of visibly discolored soil. Soils collected at depth extended to the B horizon. The visibly discolored area of soil due to carrion hotspot formation extended approximately 35-40 cm from the hotspot center along the surface and to a few centimeters depth.

Figure 2: View of a beaver after placement (a) and during advanced decay (b) to demonstrate the lateral migration of carcass-derived fluids during decay. Both photos are from the same animal, and (b) were taken during advanced decay (8 August 2016). Visible extent of fluid migration is outlined in the white dashed line.

Figure 3: Lateral changes in soil stable (a) $\delta^{15}N$ and (b) $\delta^{13}C$ isotopic composition and (c) C/N ratios extending from carrion hotspot centers. Soil was visibly discolored 35-40 cm from the center (here, 0 cm distance). Letters indicate soil samples taken at discrete distances from hotspot center that were not significantly different based on an ANOVA and Holm-Sidak post-hoc test, and asterisks denote significant differences between control and hotspot soils (t-test) at each respective distance. The dashed line represents control surface soil (0-5 cm) composition.

Figure 4: Results of linear two-member isotope mixing distinguishing the contributions of soil and carcass fluid to bulk soil stable isotopic composition.

Figure 5: Stable isotopic composition and C/N ratios for soils beneath carrion hotspots (closed circles) and at a control location (stars). Letters indicate hotspot soil samples as a function of depth that were not significantly different based on post hoc testing, and asterisks indicate significant differences between control and hotspot soils at each depth interval (both based on one-way ANOVA, $p < 0.05$).

Figure 6: Bulk soil stable isotopic composition and corresponding negative natural log %N (a) and %C (b) for hotspot and control soils with depth. Linear regressions were fit to hotspot and control datasets.

References

Aitkenhead-Peterson, J. A., Owings, C. G., Alexander, M. B., Larison, N., and Bytheway, J. A.: Mapping the lateral extent of human cadaver decomposition with soil chemistry, Forensic Sci. Int., 216, 127-134, https://doi.org/10.1016/j.forsciint.2011.09.007, 2012.

Barton, P. S., Cunningham, S. A., Lindenmayer, D. B., and Manning, A. D.: The role of carrion in maintaining biodiversity and ecological processes in terrestrial ecosystems, Oecologia, 171, 761-772, https://doi.org/10.1007/s00442-012-2460-3, 2013.

Baruzzi, C., Mason, D., and Lashley, M. A.: Effects of increasing carrion biomass on food webs, Food Webs, 16, https://doi.org/10.1016/j.fooweb/2018.e00096, 2018.

Belser, L. W., and Mays, E. L.: Specific inhibition of nitrite oxidation by chlorate and its use in assessing nitrification in soils and sediments, Appl. Environ. Microbiol., 39, 505-510, 1980.

Billings, S. A., and Richter, D. D.: Changes in stable isotopic signatures of soil nitrogen and carbon during 40 years of forest development, Oecologia, 148, 325-333, https://doi.org/10.1007/s00442-006-0366-7, 2006.

Bump, J. K., Peterson, R. O., and Vucetich, J. A.: Wolves modulate soil nutrient heterogeneity and foliar nitrogen by configuring the distribution of ungulate carcasses, Ecology, 90, 3159-3167, https://doi.org/10.1890/09-0292.1, 2009a.

Bump, J. K., Webster, C. R., Vucetich, J. A., Peterson, R. O., Shields, J. M., and Powers, M. D.: Ungulate carcasses perforate ecological filters and create biogeochemical hotspots in forest

herbaceous layers allowing trees a competitive advantage, Ecosystems, 12, 996-1007, https://doi.org/10.1007/s10021-009-9274-0, 2009b.

Carter, D. O., Yellowlees, D., and Tibbett, M.: Cadaver decomposition in terrestrial ecosystems, Naturwissenschaften, 94, 12-24, https://doi.org/10.1007/s00114-006-0159-1, 2007.

Carter, D. O., Yellowlees, D., and Tibbett, M.: Temperature affects microbial decomposition of cadavers (*Rattus rattus*) in contrasting soils, Appl. Soil. Ecol., 40, 129-137, https://doi.org/10.1016/j.apsoil.2008.03.010, 2008.

Carter, D. O., Yellowlees, D., and Tibbett, M.: Moisture can be the dominant environmental parameter governing cadaver decomposition in soil, Forensic Sci. Int., 200, 60-66, https://doi.org/10.1016/j.forsciint.2010.03.031, 2010.

Cobaugh, K. L., Schaeffer, S. M., and DeBruyn, J. M.: Functional and structural succession of soil microbial communities below decomposing human cadavers, PLoS One, https://doi.org/10.1371/journal.pone.0130201, 2015.

Danell, K., Berteaux, D., and Brathen, K. A.: Effect of muskox carcasses on nitrogen concentration in tundra vegetation, Arctic, 55, 389-392, 2002.

Doane, T. A., and Horwath, W. R.: Spectrophotometric determination of nitrate with a single reagent, Anal. Lett., 36, 2713-2722, https://doi.org/10.1081/AL-120024647, 2003.

Doyle, A., Weintraub, M. N., and Schimel, J. P.: Persulfate digestion and simultaneous colorimetric analysis of carbon and nitrogen in soil extracts, Soil Sci. Soc. Am. J., 68, 669-676, 2004.

Erskine, P. D., Bergstrom, D. M., Schmidt, S., Stewart, G. R., Tweedie, C. E., and Shaw, J. D.: Subantarctic Macquarie Island—a model ecosystem for studying animal-derived nitrogen

sources using ^{15}N natural abundance, Oecologia, 117, 187-193, https://doi.org/10.1007/S004420050647, 1998.

Evans, R. D.: Physiological mechanisms influencing plant nitrogen isotope composition, Trends Plant Sci., 6, 121-126, https://doi.org/10.1016/S1360-1385(01)01889-1, 2001.

Fox-Dobbs, K., Bump, J. K., Peterson, R. O., Fox, D. L., and Koch, P. L.: Carnivore-specific stable isotope variables and variation in the foraging ecology of modern and ancient wolf populations: case studies from Isle Royale, Minnesota, and La Brea, Can. J. Zool., 85, 458-471, https://doi.org/10.1139/Z07-018, 2007.

Gomes, L., Godoy, W. A. C., and Von Zuben, C. J.: A review of postfeeding larval dispersal in blowflies: implications for forensic entomology, Naturwissenschaften, 93, 207-215, https://doi.org/10.1007/s00114-006-0082-5, 2006.

Hart, S. C., Stark, J.M., Davidson, E.A., Firestone, M.K.: Nitrogen mineralization, immobilization, and nitrification, in: Methods of soil analysis part 2: microbiological and biochemical properties, Edited by: Weaver, R. W., Angle, S., Bottomley, P., Bezdicek, D., Smith, S., Tabatabai, A., Wollum, A., Soil Science Society of America, Madison, Wisconsin, 985-1018, 1994.

Keenan, S. W., Schaeffer, S. M., Jin, V. L., and DeBruyn, J. M.: Mortality hotspots: nitrogen cycling in forest soils during vertebrate decomposition, Soil Biol. Biochem., 121, 165-176, https://doi.org/10.1016/j.soilbio.2018.03.005, 2018a.

Keenan, S. W., Emmons, A. L., Taylor, L. S., Phillips, G., Mason, A. R., Mundorff, A., Bernard, E.C., Davoren, J., and DeBruyn, J. M.: Soil physiochemistry and microbial ecology of a multi-individual grave. PLoS One, https://doi.org/10.1371/journal.pone.0208845, 2018b.

Keeney, D. R., and Nelson, M. H.: Nitrogen—inorganic forms, in: Methods of soil analysis, part 2, chemical and microbiological methods, Edited by: Page, A. L., Miller, D. R., and Keeney, D. R., American Society of Agronomy and the Soil Science Society of America, Madison, WI, 643-698, 1982.

Kline, T. C., Goering, J. J., Mathisen, O. A., Poe, P. H., and Parker, P. L.: Recycling of elements transported upstream by runs of Pacific salmon: 1, $\delta^{15}N$ and $\delta^{13}C$ evidence in Sashin Creek, southeastern Alaska, Can. J. Fish. Aquat. Sci., 47, 136-144, https://doi.org/10.1139/F90-014, 1990.

Koyama, A., Kavanagh, K., and Robinson, A.: Marine nitrogen in central Idaho riparian forests: evidence from stable isotopes, Can. J. Fish. Aquat. Sci., 62, 518-526, https://doi.org/10.1139/F04-220, 2005.

Liang, C., Schimel, J. P., and Jastrow, J. D.: The importance of anabolism in microbial control over soil carbon storage, Nat. Microbiol., 2, https://doi.org/10.1038/Nmicrobiol.2017.105, 2017.

Lodge, D. J., Winter, D., Gonzalez, G., and Clum, N.: Effects of hurricane-felled tree trunks on soil carbon, nitrogen, microbial biomass, and root length in a wet tropical forest, Forests, 7, https://doi.org/10.3390/F7110264, 2016.

Macdonald, B. C. T., Farrell, M., Tuomi, S., Barton, P. S., Cunningham, S. A., and Manning, A. D.: Carrion decomposition causes large and lasting effects on soil amino acid and peptide flux, Soil Biol. Biochem., 69, 132-140, https://doi.org/10.1016/j.soilbio.2013.10.042, 2014.

Martinelli, L. A., Piccolo, M. C., Townsend, A. R., Vitousek, P. M., Cuevas, E., McDowell, W., Robertson, G. P., Santos, O. C., and Treseder, K.: Nitrogen stable isotopic composition of

leaves and soil: tropical versus temperate forests, Biogeochemistry, 46, 45-65, https://doi.org/10.1023/A:1006100128782, 1999.

McClain, M. E., Boyer, E. W., Dent, C. L., Gergel, S. E., Grimm, N. B., Groffman, P. M., Hart, S. C., Harvey, J. W., Johnston, C. A., Mayorga, E., McDowell, W. H., and Pinay, G.: Biogeochemical hot spots and hot moments at the interface of terrestrial and aquatic ecosystems, Ecosystems, 6, 301-312, https://doi.org/10.1007/s10021-003-0161-9, 2003.

Melis, C., Selva, N., Teurlings, I., Skarpe, C., Linnell, J. D. C., and Andersen, R.: Soil and vegetation nutrient response to bison carcasses in Białeowieża Primeval Forest, Poland, Ecol. Res., 22, 807-813, https://doi.org/10.1007/s11284-006-0321-4, 2007.

Metcalf, J. L., Parfrey, L. W., Gonzalez, A., Lauber, C. L., Knights, D., Ackermann, G., Humphrey, G. C., Gebert, M. J., Van Treuren, W., Berg-Lyons, D., Keepers, K., Guo, Y., Bullard, J., Fierer, N., Carter, D. O., and Knight, R.: A microbial clock provides an accurate estimate of the postmortem interval in a mouse model system, Elife, 2, https://doi.org/10.7554/eLife.01104, 2013.

Natelhoffer, K. J., and Fry, B.: Controls on natural ^{15}N and ^{13}C abundances in forest soil organic matter, Soil Sci. Soc. Am. J., 52, 1633-1640, 1988.

Parmenter, R. R., and Lamarra, V. A.: Nutrient cycling in a freshwater marsh: the decomposition of fish and waterfowl carrion, Limnol. Oceanogr., 36, 976-987, 1991.

Parmenter, R. R., and MacMahon, J. A.: Carrion decomposition and nutrient cycling in a semiarid shrub-steppe ecosystem, Ecol. Monogr., 79, 637-661, https://doi.org/10.1890/08-0972.1, 2009.

Payne, J. A.: A summer carrion study of the baby pig *Sus scrofa* Linnaeus, Ecology, 46, 592-602, https://doi.org/10.2307/1934999, 1965.

Putman, R. J.: Dynamics of the blowfly, *Calliphora erythrocephala*, within carrion, J. Anim. Ecol., 46, 853-866, 1977.

R core team, R: A language and environment for statistical computing: https://www.R-project.org/, version 3.5.0, 2018.

Redmile-Gordon, M. A., Armenise, E., White, R. P., Hirsch, P. R., and Goulding, K. W. T.: A comparison of two colorimetric assays, based upon Lowry and Bradford techniques, to estimate total protein in soil extracts, Soil Biol. Biochem., 67, 166-173, https://doi.org/10.1016/j.soilbio.2013.08.017, 2013.

Rhine, E. D., Sims, G. K., Mulvaney, R. L., and Pratt, E. J.: Improving the Berthelot reaction for determining ammonium in soil extracts and water, Soil Sci. Soc. Am. J., 62, 473-480, 1998.

Robinson, D.: $\delta^{15}N$ as an integrator of the nitrogen cycle, Trends Ecol. Evol., 16, 153-162, https://doi.org/10.1016/S0169-5347(00)02098-X, 2001.

Soil Survey Staff, Web Soil Survey, Natural Resources Conservation Service, United States Department of Agriculture: https://websoilsurvey.sc.egov.usda.gov/, Accessed 29 May 2018.

Szelecz, I., Koenig, I., Seppey, C. V. W., Le Bayon, R. C., and Mitchell, E. A. D.: Soil chemistry changes beneath decomposing cadavers over a one-year period, Forensic Sci. Int., 286, 155-165, https://doi.org/10.1016/j.forsciint.2018.02.031, 2018.

Towne, E. G.: Prairie vegetation and soil nutrient responses to ungulate carcasses, Oecologia, 122, 232-239, https://doi.org/10.1007/Pl00008851, 2000.

van der Waal, C., Kool, A., Meijer, S. S., Kohi, E., Heitkonig, I. M. A., de Boer, W. F., van Langevelde, F., Grant, R. C., Peel, M. J. S., Slotow, R., de Knegt, H. J., Prins, H. H. T., and de Kroon, H.: Large herbivores may alter vegetation structure of semi-arid savannas through

soil nutrient mediation, Oecologia, 165, 1095-1107, https://doi.org/10.1007/s00442-010-1899-3, 2011.

Vidon, P., Allan, C., Burns, D., Duval, T. P., Gurwick, N., Inamdar, S., Lowrance, R., Okay, J., Scott, D., and Sebestyen, S.: Hot spots and hot moments in riparian zones: potential for improved water quality management, J. Am. Water Resour. Assoc., 46, 278-298, https://doi.org/10.1111/j.1752-1688.2010.00420.x, 2010.

Wheeler, T. A., Kavanagh, K. L., and Daanen, S. A.: Terrestrial salmon carcass decomposition: nutrient and isotopic dynamics in central Idaho, Northwest Sci., 88, 106-119, https://doi.org/10.3955/046.088.0206, 2014.

Wheeler, T. A., and Kavanagh, K. L.: Soil biogeochemical responses to the deposition of anadromous fish carcasses in inland riparian forests of the Pacific Northwest, USA, Can. J. Forest Res., 47, 1506-1516, https://doi.org/10.1139/cjfr-2017-0194, 2017.

Wright, S. F., and Upadhyaya, A.: Extraction of an abundant and unusual protein from soil and comparison with hyphal protein of arbuscular mycorrhizal fungi, Soil Sci., 161, 575-586, https://doi.org/10.1097/00010694-199609000-00003, 1996.

Table 1: Selected soil biogeochemical data during one year of decomposition. Letters indicate hotspot soil samples within each measured dataset (i.e., pH) that were not significantly different based on One-way ANOVA ($p < 0.05$) and Holm-Sidak post-hoc testing. Asterisks indicate significant differences between control and treatment soils. N.M. indicates parameters were not measured. Control samples were homogenized into a single representative sample and do not have standard deviations. Data, except for bolded 1 yr. post decay, were previously published in Keenan et al. (2018a).

	Sampling Date	**Soil Gravimetric Moisture**	**pH**	**Conductivity (µS cm^{-1})**	**Dissolved Oxygen (%)**	**Total carbon (%)**	**Total nitrogen (%)**	**C/N**	**δ^{15}N**	**δ^{13}C**
Initial	29 July	0.299 ± 0.012^{AB}	6.79 ± 0.1^{A}	47.83 ± 5.9^{AC}	98.5 ± 0.29^{A}	5.11 ± 0.101	0.295 ± 0.009	17.33 ± 0.25^{AC}	1.48 ± 0.23^{A}	-27.86 ± 0.08
Early	1 August	0.216 ± 0.034^{A}	6.86 ± 0.3^{A}	73.53 ± 32.2^{A}	N.M.	3.927 ± 1.08	0.245 ± 0.058	15.93 ± 1.7^{AC}	2.65 ± 1.66^{A}	-27.73 ± 0.42
Early control	1 August	0.219	6.82	36.78	N.M.	4.196	0.247	16.99	1.76	-27.56
Active	3 August	0.234 ± 0.056^{A}	8.64 ± 0.3^{B}	2150.48 ± 1282^{BC}	9.16 ± 7.89^{BC}	4.251 ± 0.798	0.362 ± 0.096	12.01 ± 1.34^{BC}	6.23 ± 1.50^{B}	-27.77 ± 0.30
Active control	3 August	0.160	6.68*	31.65*	98.6 ± 1.25*	4.159	0.267	15.58*	1.48*	-27.68
Advanced	9 August	0.286 ± 0.081^{AB}	8.78 ± 0.1^{B}	1233 ± 494^{C}	19.4 ± 31.2^{B}	4.000 ± 1.29	0.303 ± 0.080	13.07 ± 0.75^{BC}	8.72 ± 2.09^{B}	-27.64 ± 0.20
Advanced control	9 August	0.223	6.84*	43.42*	98.0 ± 0.57*	5.008	0.281	17.82*	1.26*	-27.77
Early skeletal	6 September	0.242 ± 0.070^{A}	7.58 ± 0.4^{C}	973.8 ± 211^{AC}	97.4 ± 0.84^{AC}	3.610 ± 0.839	0.293 ± 0.057	12.28 ± 0.74^{BC}	9.26 ± 1.54^{B}	-27.74 ± 0.30
Early skeletal control	6 September	0.121	6.84*	35.08	98.3 ± 0.50	4.023	0.259	15.53*	1.78*	-27.63
Late skeletal	9 December	0.271 ± 0.021^{AB}	6.93 ± 0.3^{A}	225.2 ± 84.8^{AC}	100 ± 0^{A}	2.668 ± 0.352	0.214 ± 0.030	12.51 ± 0.67^{BC}	9.25 ± 1.33^{B}	-27.41 ± 0.25
Late skeletal control	9 December	0.246	6.73	29.13	100 ± 0	2.084	0.136	15.37*	1.79*	-27.30
1 yr. post decay	**10 August**	**0.404 ± 0.027^{B}**	**6.10 ± 0.3^{D}**	**29.47 ± 7.6^{A}**	**N.M.**	**4.253 ± 1.07**	**0.285 ± 0.036**	**15.24 ± 3.49^{C}**	**8.42 ± 1.52^{B}**	**-27.67 ± 0.25**

1 yr. post decay control	**10 August**	**0.449***	**6.29***	**23.07**	**N.M.**	**4.36**	**0.26**	**17.08**	**0.05***	**-27.73**

Table 1 (continued):

	Protein (mg g^{-1})	**Microbial respiration rate (µg CO_2-C release gdw^{-1} day^{-1})**	**DOC (µg C gdw^{-1})**	**Ammonium (mg NH_4-N gdw^{-1})**	**Nitrification potential rate (mg NO_2 gdw^{-1} day^{-1})**	**Nitrate (mg NO_3^--N gdw^{-1})**	**DON (mg N gdw^{-1})**	**Accumulated Degree Days (ADD)**
Initial	0.251 ± 0.051	50.9 ± 8^{A}	2.44 ± 0.2^{AC}	0.039 ± 0.01^{A}	0.181 ± 0.05^{A}	0.000 ± 0.0^{A}	0.283 ± 0.02^{A}	26.1
Early	0.200 ± 0.037	51.4 ± 18^{A}	3.44 ± 1.0^{A}	0.101 ± 0.06^{A}	0.237 ± 0.16^{A}	0.000 ± 0.0^{A}	0.718 ± 0.35^{A}	106.7
Early control	0.159 ± 0.004	35.2	2.35	0.011	0.167	0.000	0.242	106.7
Active	0.260 ± 0.025	300 ± 90^{B}	66.54 ± 40.4^{B}	2.49 ± 1.24^{B}	0.366 ± 0.09^{A}	0.001 ± 0.0^{A}	1.363 ± 1.4^{A}	160.3
Active control	0.225 ± 0.007	27.8*	2.52*	0.010*	0.163	0.000	0.205	160.3
Advanced	0.281 ± 0.072	162.8 ± 110^{A}	42.5 ± 30.0^{C}	2.29 ± 1.80^{BC}	0.517 ± 0.17^{A}	0.001 ± 0.0^{A}	1.906 ± 1.7^{A}	321.7
Advanced control	0.239 ± 0.024*	45.7*	3.44*	0.015*	0.181	0.003	0.304	321.7
Early skeletal	0.238 ± 0.049	76.9 ± 42^{A}	14.3 ± 3.4^{AC}	0.775 ± 0.14^{AC}	8.57 ± 4.4^{B}	0.309 ± 0.169^{B}	6.089 ± 1.24^{B}	1042.8
Early skeletal control	0.193 ± 0.021	20.8	2.89	0.006	0.130*	0.000*	0.185*	1042.8
Late skeletal	0.250 ± 0.014	57.2 ± 26^{A}	10.2 ± 8.4^{AC}	0.246 ± 0.06^{A}	0.017 ± 0.20^{A}	0.019 ± 0.001^{A}	1.929 ± 0.37^{A}	2591.7
Late skeletal control	0.195 ± 0.016	46.5	3.12	0.012	0.039	0.000	0.309	2591.7
1 yr. post decay	**0.239 ± 0.021**	**64.1 ± 8^{A}**	**2.81 ± 0.5^{A}**	**0.008 ± 0.0^{A}**	**0.006 ± 0.00^{A}**	**0.001 ± 0.0^{A}**	**0.095 ± 0.01^{A}**	**6377.5**
1 yr. post decay control	**0.195 ± 0.008**	**59.5**	**2.43 ± 0.0**	**0.007**	**0.006**	**0.000**	**0.093**	**6377.5**

Table 2: Differences in soil $\delta^{15}N$ at depth and $\delta^{15}N$ in surface soils for hotspot and control depth profiles.

	$\Delta^{15}N$ (‰)	
Depth (cm)	**Hotspot**	**Control**
0	0	0
5	-2.1	2.65
10	-1.5	3.2
15	0.1	6.6
20	0.9	7.7
30	0.9	6.1
40	1.2	8.4

545

Figure 1

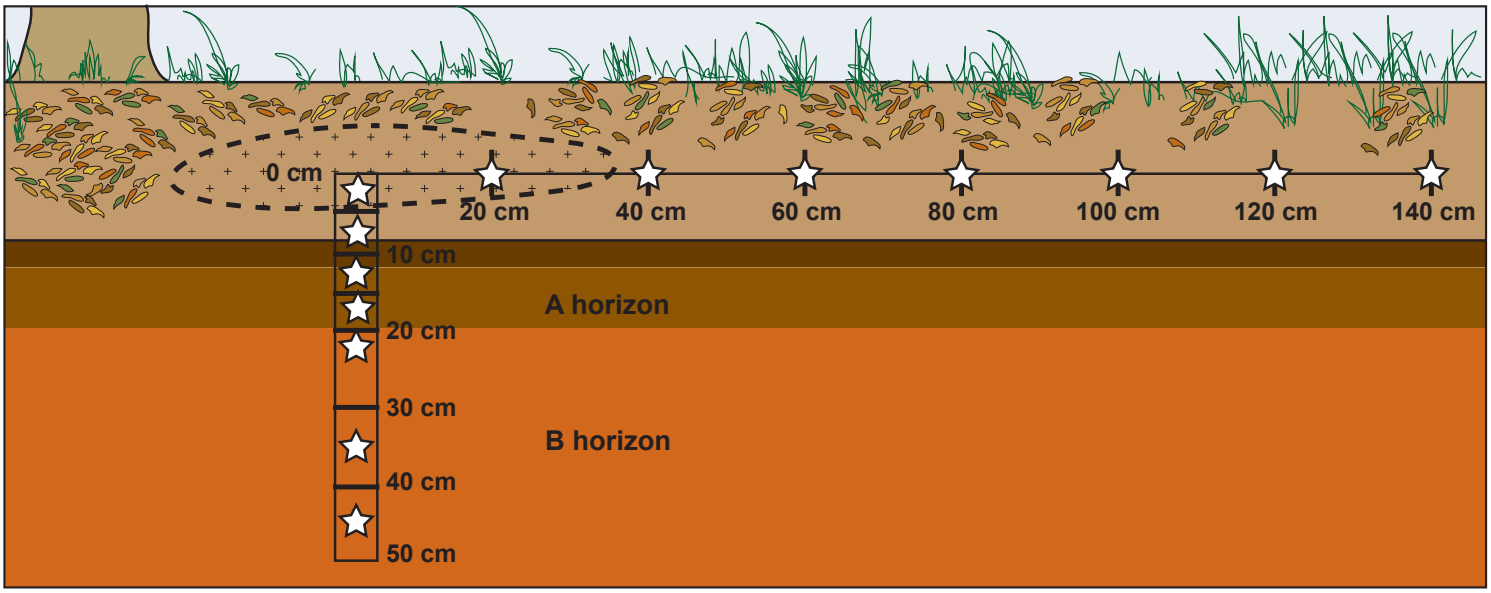
0 cm
20 cm
40 cm
60 cm
80 cm
100 cm
120 cm
140 cm
10 cm
A horizon
20 cm
30 cm
B horizon
40 cm
50 cm

Figure 2

Figure 3

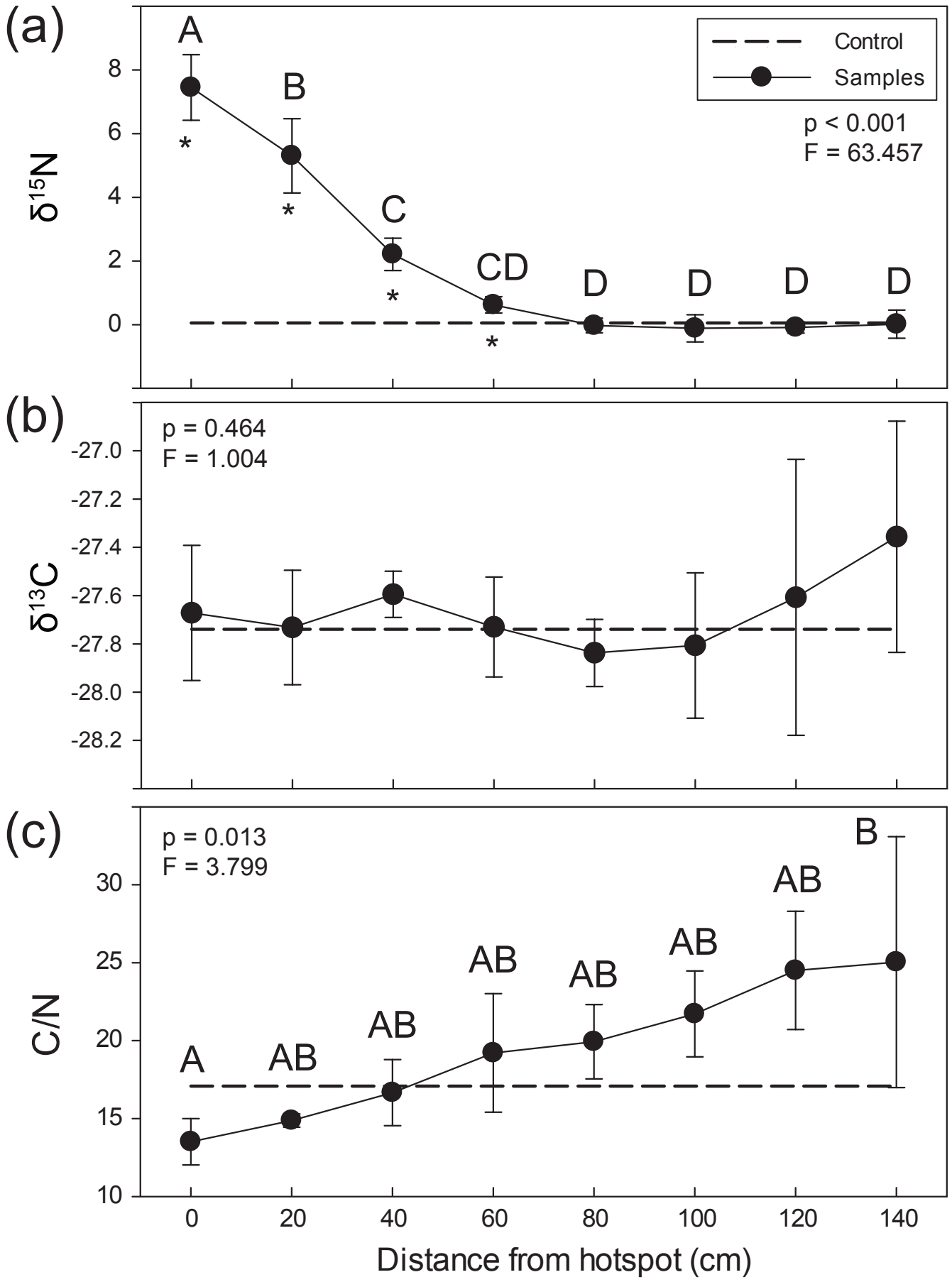
(a)
A
B
C
CD
D
D
D
D
*
*
*
*
Control
Samples
p < 0.001
F = 63.457
δ15N
8
6
4
2
0
(b)
p = 0.464
F = 1.004
δ13C
-27.0
-27.2
-27.4
-27.6
-27.8
-28.0
-28.2
(c)
p = 0.013
F = 3.799
C/N
A
AB
AB
AB
AB
AB
B
30
25
20
15
10
0
20
40
60
80
100
120
140
Distance from hotspot (cm)

Figure 4

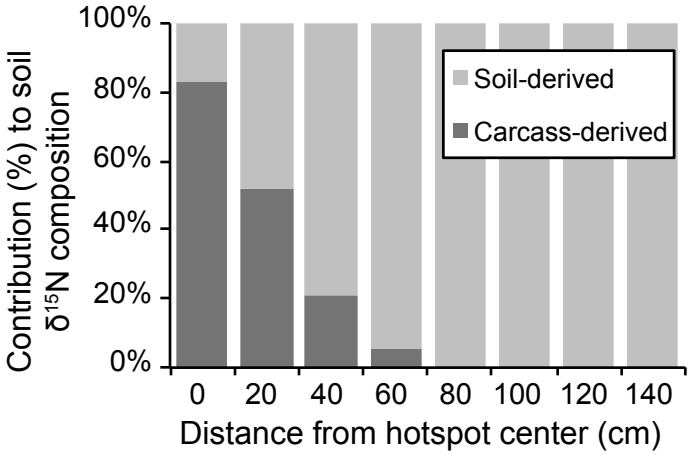
100%
80%
60%
40%
20%
0%
Contribution (%) to soil
δ15N composition
Soil-derived
Carcass-derived
0
20
40
60
80
100
120
140
Distance from hotspot center (cm)

Figure 5

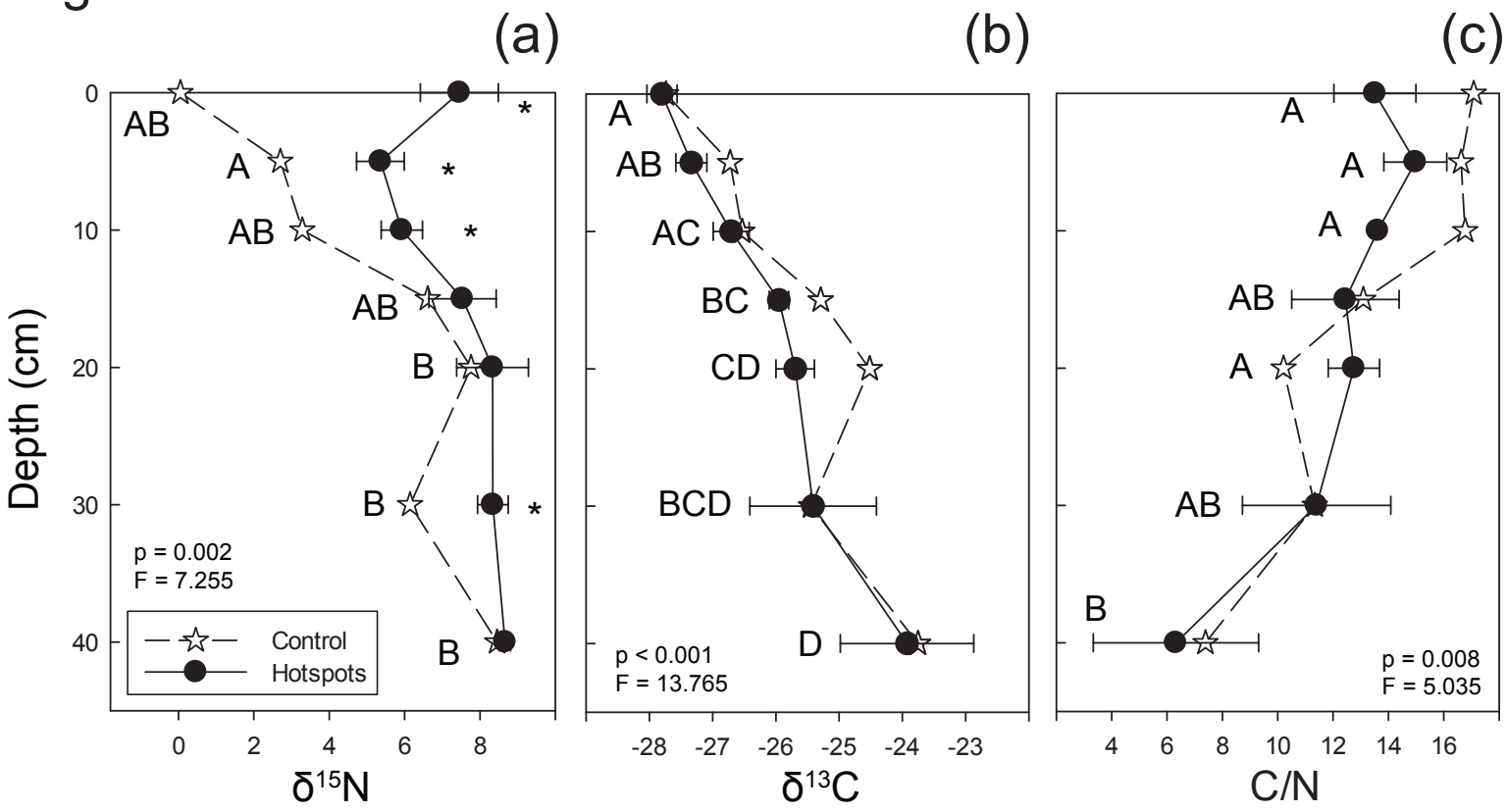
(a)
(b)
(c)
Depth (cm)
0
10
20
30
40
AB
A
AB
AB
B
B
B
*
*
*
*
p = 0.002
F = 7.255
Control
Hotspots
0
2
4
6
8
δ15N
A
AB
AC
BC
CD
BCD
D
p < 0.001
F = 13.765
-28
-27
-26
-25
-24
-23
δ13C
A
A
A
AB
A
AB
B
p = 0.008
F = 5.035
4
6
8
10
12
14
16
C/N

Figure 6

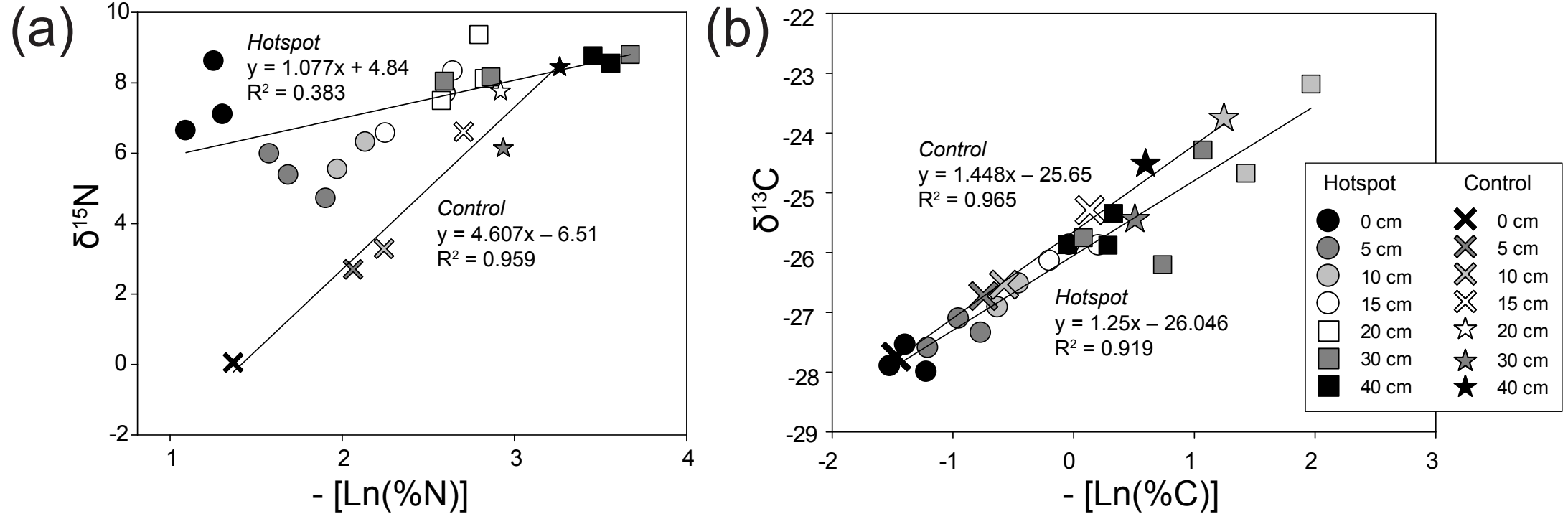
(a)
Hotspot
y = 1.077x + 4.84
R² = 0.383
Control
y = 4.607x – 6.51
R² = 0.959
δ15N
- [Ln(%N)]
(b)
Control
y = 1.448x – 25.65
R² = 0.965
Hotspot
y = 1.25x – 26.046
R² = 0.919
δ13C
- [Ln(%C)]
Hotspot
Control
0 cm
5 cm
10 cm
15 cm
20 cm
30 cm
40 cm